nature neuroscience

The transmembrane semaphorin Sema6A controls cerebellar granule cell migration

Géraldine Kerjan[1], Jackie Dolan[2], Cécile Haumaitre[3], Sylvie Schneider-Maunoury[3], Hajime Fujisawa[4], Kevin J Mitchell[2] & Alain Chédotal[1]

The transmembrane semaphorin protein Sema6A is broadly expressed in the developing nervous system. Sema6A repels several classes of developing axons *in vitro* and contributes to thalamocortical axon guidance *in vivo*. Here we show that during cerebellum development, Sema6A is selectively expressed by postmitotic granule cells during their tangential migration in the deep external granule cell layer, but not during their radial migration. In Sema6A-deficient mice, many granule cells remain ectopic in the molecular layer where they differentiate and are contacted by mossy fibers. The analysis of ectopic granule cell morphology in *Sema6a*$^{-/-}$ mice, and of granule cell migration and neurite outgrowth in cerebellar explants, suggests that Sema6A controls the initiation of granule cell radial migration, probably through a modulation of nuclear and/or soma translocation. Finally, the analysis of mouse chimeras suggests that this function of Sema6A is primarily non-cell-autonomous.

In the vertebrate central nervous system (CNS), cerebellar granule cell precursors generated in the embryonic rhombic lips migrate tangentially over the cerebellar plate to form the external granular layer (EGL)[1]. In rodents, this secondary germinative zone produces granule cells only after birth[2]. In the deeper part of the EGL, postmitotic granule cells migrate tangentially in all directions[2,3] and undergo a series of profound morphological changes[4]. They first extend a process horizontally, which is soon followed by a second one extending in the opposite direction, before a third process develops perpendicular to the surface. This precedes the inward radial migration of granule cell bodies, along Bergmann glia fibers[5] to the internal granular layer (IGL, **Fig. 1a**). The horizontal processes become the granule cell axons known as parallel fibers. The radial migration of granule cells has been extensively studied (see ref. 5 for a review), but much less is known about the molecules that control their tangential migration or the switch from tangential to radial migration[5].

Semaphorins are secreted or membrane-bound proteins that control axon guidance and cell migration[6]. Many, if not all, transmembrane semaphorins are expressed in the developing CNS, but little is known of their functions *in vivo*. Class 6 semaphorins comprise four proteins, Sema6A–Sema6D, that are closely related to invertebrate transmembrane semaphorins[6]. Class 6 semaphorins can collapse various classes of axons[7–9]; this process seems to be mediated by receptors of the plexin-A family[9,10]. Class 6 semaphorins and the related insect class 1 semaphorins[6,11] are also capable of bidirectional signaling, apparently acting as receptors in certain contexts[10,12]. Recently, a mouse line deficient in Sema6A was obtained using a gene-trapping strategy[13,14]. Sema6A-deficient mice have abnormalities in several axonal tracts, including thalamocortical projections[13]. Here we show that in the developing cerebellum, Sema6A may control the initiation of granule cell radial migration, probably by influencing nucleus or soma translocation in a non-cell-autonomous manner.

RESULTS

Sema6A is transiently expressed in the deeper EGL

Sema6A messenger RNAs (mRNAs) were detected in the EGL of the E15–E17 embryonic mouse cerebellum as previously described (data not shown and ref. 15). In the postnatal cerebellar cortex, Sema6A transcripts were found in the deeper EGL and in the IGL (**Fig. 1b**). To localize Sema6A protein, we used monoclonal and polyclonal antibodies directed against ectodomains of the human or mouse Sema6A (amino acids 19–649). On western blots of cell extracts collected from COS7 cells transfected with plasmids encoding full-length Sema6A (see Methods), these antibodies recognized a band at the expected molecular weight (120 kDa) but did not recognize other class 6 semaphorins (data not shown).

To confirm the specificity of Sema6A antibodies, we labeled sections from postnatal day (P) 10 *Sema6a*$^{-/-}$ mice[13]. These mutant mice carry a gene-trap insertion in the Sema6A gene that results in the fusion of a portion of the extracellular region of Sema6A to the reporter gene TM-ß-geo (see Methods). Such fusion proteins are sequestered intracellularly, probably in the endoplasmic reticulum, reliably producing phenotypic null alleles[14]. In the cerebellum of *Sema6a*$^{-/-}$mice, Sema6A immunostaining differs from that in wild-type mice. Subcellular Sema6A-positive dots were observed in the cerebellar cortex (**Fig. 1c**), most likely corresponding to vesicles of the endoplasmic

[1]Centre National de la Recherche Scientifique UMR7102, Université de Paris 6, Case 12, 9 Quai Saint-Bernard, 75005 Paris, France. [2]Smurfit Institute of Genetics, Trinity College Dublin, Dublin 2, Ireland. [3]Centre National de la Recherche Scientifique UMR7622, Université de Paris 6, Batiment C, Case 24, 9 Quai Saint-Bernard, 75005 Paris, France. [4]The 21st Century Center of Excellence Program, Division of Biological Science, Nagoya University Graduate School of Science, Chikusa-ku, Nagoya 464–8602, Japan. Correspondence should be addressed to A.C. (chedotal@infobiogen.fr).

Received 11 July; accepted 31 August; published online 2 October 2005; doi:10.1038/nn1555

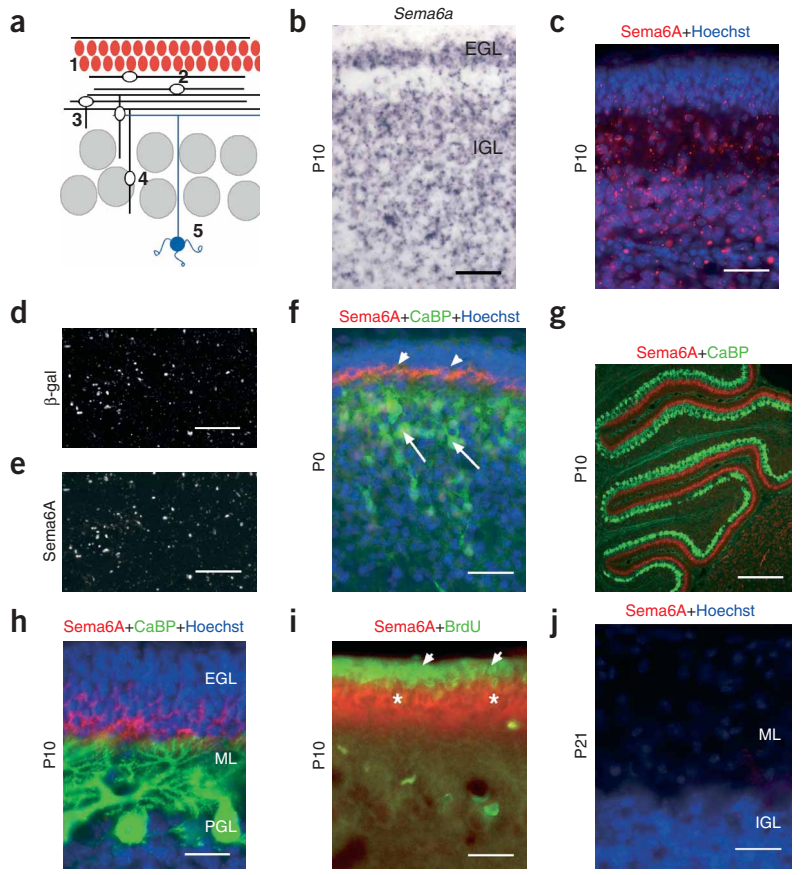

Figure 1 Sema6A is expressed in tangentially migrating granule cells. (**a**) Phases of granule cell development. (1) Granule cell precursors proliferate in the outer portion of the external granule cell layer (EGL). (2) Postmitotic granule cells in the deeper EGL extend two horizontal processes and migrate tangentially. They next send a third process perpendicular (3) and migrate radially through the molecular layer and Purkinje cell layer (grey circles) along radial glia (4) to settle in the internal granule cell layer or IGL (5). (**b**) At P10, *Sema6a* mRNAs are expressed in the deeper EGL and in the IGL. (**c**) Cerebellum section from P10 *Sema6Aa*$^{-/-}$ mouse. In contrast with the wild-type (see **h**), Sema6A immuno-positive dots are observed throughout the EGL, molecular layer and IGL. (**d**,**e**) 1-μm confocal image of the cerebellar cortex of a P10 *Sema6a*$^{-/-}$ mouse, double labeled with antibodies to Sema6A (in **e**) and anti-β-galactosidase (in **d**) antibodies, showing that Sema6A and β-gal are co-expressed, most likely in small intracytoplasmic vesicles. (**f**) At P0, Sema6A expression is restricted to the deeper EGL (arrowheads) above CaBP-positive Purkinje cells (arrows). (**g**,**h**) P10 cerebellum section immunostained with antibody to Sema6A and CaBP with Hoechst counterstaining. Sema6A is still restricted to the deeper EGL. (**i**) Sema6A immunoreactive granule cells (asterisks) are immediately adjacent to the upper EGL containing proliferating BrdU-labeled granule cell precursors (arrowheads). (**j**) At P21, Sema6A is not expressed in the cerebellar cortex. Scale bars, 50 μm (**b**,**c**,**f**,**j**), 500 μm (**g**), 35 μm (**d**,**e**,**h**,**i**).

reticulum. Confocal microscopy showed that Sema6A-positive dots coexpressed β-galactosidase (**Fig. 1d**,**e**) as expected for a fusion protein.

From birth to P10, Sema6A immunoreactivity was observed in the deeper EGL as shown on sections double stained with the Purkinje cell marker calbindin D28k[16] (**Fig. 1f–h** and data not shown). At P10, BrdU-positive proliferating granule cell precursors in the upper EGL were Sema6A negative (**Fig. 1i**). Also, radially migrating granule cells in the molecular layer and postmigratory granule cells in the IGL were not immunoreactive to Sema6A, although they expressed Sema6A mRNA, indicating a precise translational regulation of Sema6A expression. At P21, when granule cell proliferation and migration had stopped[17], Sema6A immunoreactivity was no longer detected in the molecular layer or IGL (**Fig. 1j**).

Arrested granule cell migration in Sema6A-deficient mice

To determine the function of Sema6A in granule cell development, we analyzed mice genetically engineered to be deficient in Sema6A[13]. *Sema6a*$^{-/-}$ mice are viable and fertile and do not show any substantial behavioral defects (data not shown). The gross anatomy of the cerebellum from *Sema6a*$^{-/-}$ mice was indistinguishable from that of the wild type (data not shown).

In sections from wild-type mice and *Sema6a*$^{+/-}$ stained with cresyl violet, the adult cerebellar cortex had its typical regular organization (**Fig. 2a**,**b**). In Sema6A-deficient mice (**Fig. 2c**,**d**), Purkinje cells and molecular layer interneurons showed normal distribution and density, but the size of the IGL was reduced by 10%. Moreover, in all folia, numerous cells with a small, dense nucleus were found in the molecular layer, sometimes clustered at the cerebellar surface (**Fig. 2d**). To determine whether they corresponded to granule cells, sections from adult cerebellum were labeled with antibody to the granule cell–specific α6 $GABA_A$ receptor subunit (α6)[18]. In all cases, *Sema6a*$^{+/-}$ mice were identical to wild-type mice. In the wild type, α6 is expressed only by granule cells that have reached the IGL (**Fig. 2e**,**g** and ref. 18). In contrast, in *Sema6a*$^{-/-}$ mice, a large proportion of α6-positive neurons was found either within the molecular layer or aggregated in clusters under the pial surface (**Fig. 2f**,**h**). These ectopic cells also expressed Ca^{2+}/calmodulin-dependent protein kinase IV (CaMKIV), another marker of mature postmigratory granule cells[19] (data not shown; discussed below). Quantification of CaMKIV-positive granule cells indicated that about 40% remained in the molecular layer. The same results were obtained using Sema6A knockout mice 1 year of age (data not shown), indicating that the migration is not simply delayed and that the ectopic granule cells survive. The differentiation of Purkinje cells—the postsynaptic partner of granule cells—as visualized with antibodies to CaBP or zebrin II (ref. 20) or with BDA labeling (see Methods), did not seem to be affected (**Fig. 2g**,**h** and data not shown). The number of molecular-layer interneurons, as determined by Hoechst staining and parvalbumin immunostaining, was also comparable to that in the wild type (**Fig. 2g**,**h** and data not shown).

To further study the granule cell migration defect in Sema6A-deficient mice, we performed pulse labeling of migrating granule cells with BrdU (see Methods). At 108 h after a single BrdU injection, about 90% of BrdU labeled cells were found in the IGL in wild-type mice (**Supplementary Fig. 1** online), whereas 40% of the BrdU-labeled cells were still in the molecular layer in *Sema6Aa*$^{-/-}$ mice (**Supplementary**

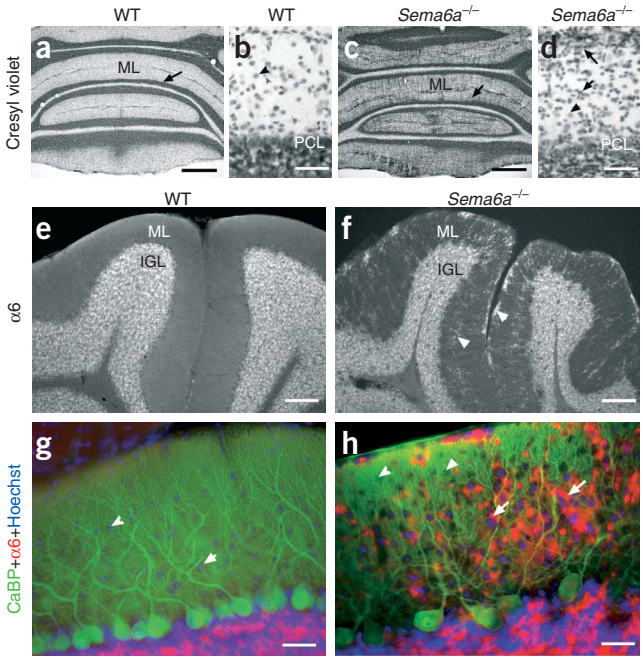

Figure 2 Abnormal granule cell migration in Sema6A-deficient mice. (**a**–**d**) Cresyl violet staining of cerebellum sections from adult wild-type (**a**,**b**) or *Sema6a*$^{-/-}$ (**c**,**d**) mice. In the wild-type (wt) cerebellum, the border between the molecular and Purkinje cell layers is sharp (arrow in **a**). In contrast, in *Sema6a*$^{-/-}$ mice this border is irregular and fuzzy (arrow in **c**; see also **d**). Moreover, cell density is higher in the molecular layer (ML) of *Sema6a*$^{-/-}$. The density of molecular layer interneurons (arrowhead in **b** and **d**) is similar, but there are many cells with small and dense nuclei (arrows in **d**) dispersed in the molecular layer of *Sema6a*$^{-/-}$ mice or accumulated near the pial surface. (**e**,**f**) Adult cerebellum sections immunostained for α6. In *Sema6a*$^{+/-}$, all α6-immunoreactive granule cells are found in the IGL and none in the molecular layer (ML), whereas in *Sema6a*$^{-/-}$, many ectopic α6-positive granule cells are found in the ML and near the pial surface (arrowheads in **f**). (**g**,**h**) Adult cerebellum section double stained for CaBP and α6 with Hoechst counterstaining. In *Sema6a*$^{+/-}$, the molecular and Purkinje cell layers do not contain α6-immunoreactive cells. The nuclei of stellate and basket cells can be observed with Hoechst in the molecular layer (arrowheads in **g**). In *Sema6a*$^{-/-}$ mice, numerous α6-positive granule cells are found in the molecular layer (arrows in **h**). Interneurons are also observed (arrowheads in **h**). Scale bars, 450 μm (**a**,**c**), 45 μm (**b**,**d**), 135 μm (**e**,**f**), 35 μm (**g**,**h**).

Fig. 1). Overall, these results suggest that granule cell migration within the EGL or from the EGL is perturbed in *Sema6a*$^{-/-}$ mice.

Granule cell proliferation, differentiation and survival

Although Sema6A is already expressed during the first phase of tangential migration of granule cell precursors, *in situ* hybridization with the granule cell precursor markers *Math1* (also known as *Atoh1* and *HATH1*) and *Barhl1* (ref. 21) showed that the EGL was indistinguishable in newborn *Sema6a*$^{+/-}$ and *Sema6a*$^{-/-}$ mice (**Supplementary Fig. 2** online). This suggests that the early migration of granule cell precursors is normal.

We quantified granule cell proliferation in P0, P10 and P21 cerebella using BrdU (see Methods) and antibodies to phospho-histone-H3. In Sema6A-deficient mice, the number of proliferating granule cells (± s.e.m.; errors are stated as s.e.m. throughout) in the upper EGL (0.025 ± 0.005 cells per μm of EGL length at P0 and 0.069 ± 0.003 cells per μm at P10) was similar to that in heterozygous mice (0.024 ± 0.001 cells per μm of EGL length at P0 and 0.058 ± 0.005 cells per μm at P10; data not shown). Moreover, by P21, no proliferating cells were detected in the molecular layer in Sema6A-deficient mice, demonstrating that the timing and level of granule cell proliferation were also normal. In the mouse cerebellum, the peak of apoptosis occurs around P8–P10 (ref. 22). To measure the level of apoptosis in the developing cerebellum, we used antibody to activated caspase-3 (ref. 23). No significant ($P > 0.05$) difference was observed in P8 Sema6A-deficient mice (**Fig. 3a**,**b**).

During their differentiation, granule cells are known to sequentially express different genes, such as the transcription factors Math1 and Pax6 (ref. 21). The expression patterns of these two genes were normal in Sema6A-deficient mice (**Fig. 3c**,**d** and data not shown). Likewise, the expression patterns of TAG-1 and L1, two molecules involved in granule cell radial migration[24,25], were normal (**Fig. 3e**–**h**).

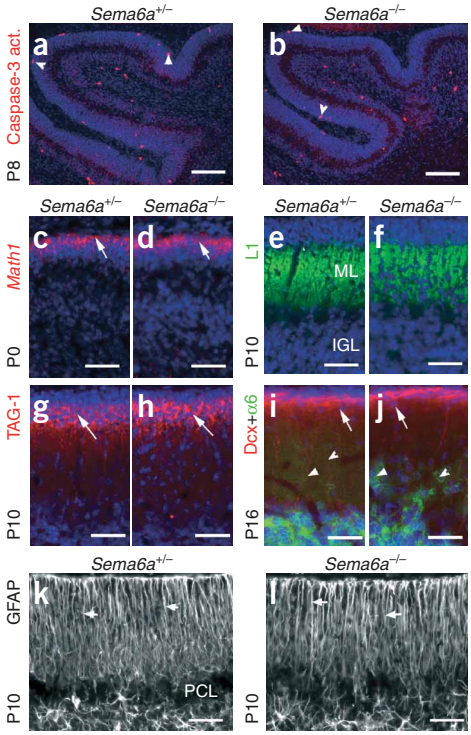

Figure 3 Normal apoptosis, differentiation and radial glia organization in Sema6A knockouts. (**a**–**l**) Sagittal cerebellum sections from *Sema6a*$^{+/-}$ (**a**,**c**,**e**,**g**,**i**,**k**) or *Sema6a*$^{-/-}$ (**b**,**d**,**f**,**h**,**j**,**l**) mice were immunostained with antibodies against activated caspase-3 (**a**,**b**), L1 (**e**,**f**), doublecortin (Dcx; **i**,**j**), TAG-1 (**g**,**h**) or GFAP (**k**,**l**) or hybridized with *Math1* riboprobes (**c**,**d**) and counterstained with Hoechst (**a**–**j**). At P8, the number of caspase-3–labeled cells in the EGL (arrowheads in **a** and **b**) is similar in *Sema6a*$^{+/-}$ (3.9 ± 0.1 cells per mm of EGL length) and *Sema6a*$^{-/-}$ (3.8 ± 0.5 cells/ per mm of EGL length). In **c** and **d**, *Math1* signal has been artificially colored in red using Photoshop and superimposed on the Hoechst labeling (in blue). There is no difference in *math1* expression between *Sema6a*$^{-/-}$ and *Sema6a*$^{+/-}$. At P10, L1 (**e**,**f**) and TAG-1 (**g**,**h**) expression patterns are identical in *Sema6a*$^{+/-}$ and *Sema6a*$^{-/-}$. In **i** and **j**, sections from P16 cerebellum are double stained for Dcx and α6. In both *Sema6a*$^{+/-}$ and *Sema6a*$^{-/-}$, Dcx is expressed in the deep EGL (arrow in **i** and **j**) and in perpendicular processes of radially migrating granule cells in the molecular layer (arrowheads in **i** and **j**). In *Sema6a*$^{-/-}$, many α6 positive cells are found in the molecular layer. At P10, the radial organization of GFAP-positive Bergmann glia cells (arrows in **k** and **l**) is similar in *Sema6a*$^{+/-}$ and *Sema6a*$^{-/-}$. Scale bars, 115 μm (**a**,**b**), 55 μm (**c**,**d**), 30 μm (**e**–**l**).

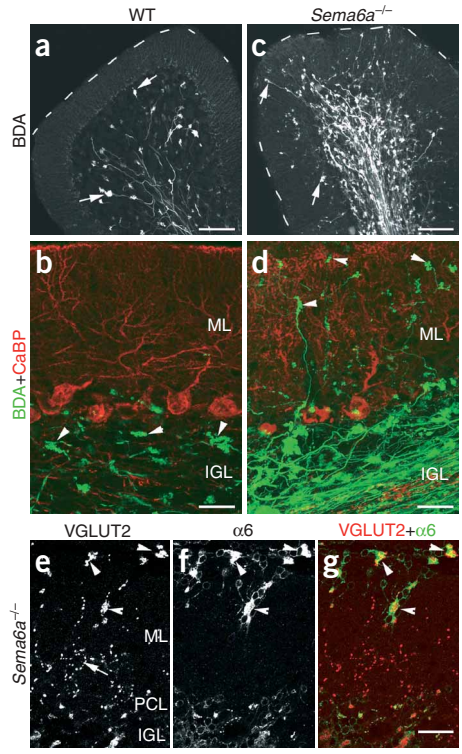

Figure 4 Ectopic granule cells are contacted by mossy fibers in *Sema6a*$^{-/-}$. (**a**–**d**) Wild-type (**a**,**b**) and *Sema6a*$^{-/-}$ (**c**,**d**) adult mice were injected into the cerebellum with BDA. Some sections (**b**,**d**) were also immunostained with antibody to CABP to label Purkinje cells. The dashed line in **a** and **c** delineates the pial surface. In wild-type (**a**,**b**), all large mossy fiber terminals (or rosettes) are located in the internal granular layer (IGL; arrows in **a** and arrowheads in **b**). No rosette is observed in the molecular layer (ML). By contrast, in *Sema6a*$^{-/-}$ (see **c**,**d**), many rosettes are detected in the ML (arrows in **c** and arrowheads in **d**), in addition to the IGL. (**e**–**g**) 1-μm confocal images of VGLUT2 and α6 double immunostaining on *Sema6a*$^{-/-}$ cerebellum. VGLUT2 labels large mossy fiber rosette (arrowheads in **e** and **g**) and punctate climbing fiber terminals (arrow in **e**). Mossy fiber rosettes contact ectopic α6-positive granule cells (arrowheads in **f** and **g**). Scale bars, 100 μm (**a**,**c**), 35 μm (**b**,**d**), 45 μm (**e**–**g**).

Doublecortin expression in radially migrating granule cells was also identical[26] (**Fig. 3i**,**j**). Finally, ectopic granule cells still expressed markers of mature granule cells such as α6 and CaMKIV (**Fig. 3i**,**j**; and data not shown).

Granule cell migration defects in *Sema6a*$^{-/-}$ mice could be due to abnormal Bergmann glia. This seemed unlikely, however, as Sema6A is expressed in tangentially migrating granule cells in the EGL, but not in radially migrating granule cells or in Bergmann glia fibers. Immunostaining of the P10 cerebellum by glial fibrillary acidic protein (GFAP) confirmed that the number, disposition and morphology of Bergmann glia fibers in *Sema6a*$^{-/-}$ mice were similar to those in *Sema6a*$^{+/-}$ mice (**Fig. 3k**,**l**). Thus the defects in migration seemed to be intrinsic to granule cells.

In wild-type mice, granule cells in the IGL establish synaptic contact with mossy fibers[27]. The large mossy fiber terminals are called 'rosettes'. To label mossy fibers, we injected BDA into the adult cerebellum of wild-type and Sema6A-deficient mice (**Fig. 4a–d**). In the wild type, BDA-labeled mossy fibers were confined to the IGL (**Fig. 4a**,**b**). In contrast, in Sema6A-deficient mice, BDA-labeled mossy fibers were also observed in the molecular layer where they formed typical rosettes (**Fig. 4c**,**d**). In addition, rosettes can be visualized using immunocytochemistry for the vesicular glutamate transporter VGLUT2 (ref. 28; **Fig. 4e**). VGLUT2 staining also labels climbing fibers (**Fig. 4e**), but the size and morphology of the two types of terminals are clearly distinguishable. VGLUT2-positive rosettes were found in the molecular layer (**Fig. 4e**) close to ectopic α6-immunopositive granule cells (**Fig. 4e–g**). Overall, these results strongly suggest that granule cell differentiation and maturation are normal in Sema6A-deficient mice.

Normal parallel fiber extension and granule cell polarity

To further understand the role of Sema6A in granule cell migration, we labeled individual granule cells and their axons (the parallel fibers) with BDA. All parallel fibers extend along the mediolateral axis of the cerebellar cortex[29]. In adult wild-type mice, BDA injection in the molecular layer labeled parallel fibers running across the entire length of the injected folia and granule cell bodies in the IGL (**Fig. 5a**). In Sema6A-deficient mice, BDA also labeled parallel fibers throughout the injected lobule, but BDA-labeled granule cells were observed in the molecular layer in addition to the IGL (**Fig. 5b**). At higher magnification, the morphology of ectopic granule cell was clearly visible (**Fig. 5c–h**). Two main categories of cells were observed. The first type was found throughout the molecular layer (**Fig. 5c**,**e**,**h**). These cells extended a process resembling mature granule cell dendrites toward the IGL, and additional dendritic processes emerged from the cell body. These processes were immunoreactive for α6, which is expressed only on granule cell bodies and dendrites[18] (**Fig. 5f–h**). These ectopic granule cells had a regular T shape[3], extending a thinner process toward the pial surface (not immunoreactive for α6) from which the parallel fiber emerged. The length of this upward process was comparable for all ectopic granule cells. The second type of cell was found near the pial surface within the α6-immunoreactive clusters (see **Fig. 2f**). These cells had a rather bipolar shape (**Fig. 5d**,**e**) with parallel fibers emerging directly from the cell body, but they also had dendritic processes, one of which was oriented toward the IGL.

Abnormal *in vitro* migration of *Sema6a*$^{-/-}$ granule cells

To determine whether Sema6A controls granule cell neurite outgrowth, we seeded dissociated granule cells from the cerebellum of P5 wild-type mice onto Sema6A-expressing COS7 cells and onto mock-transfected cells. Cultures were labeled after 24 h, using phalloidin and β-tubulin immunostaining. In Sema6A-expressing cells, the total neuritic length (length of the longest neurite) and the number of branch points were not significantly different ($P > 0.5$) from those in the controls (**Supplementary Fig. 3** online). Thus, exogenous Sema6A does not influence the elongation of granule cell neurites. We next compared the growth of cerebellar granule cell neurites in wild-type and *Sema6a*$^{-/-}$ mice. We found that neurite outgrowth from *Sema6a*$^{-/-}$ granule cells was normal. The total neuritic length and the length of the longest neurite (137.3 ± 6.9 μm and 100.3 ± 4.8 μm, respectively; $n = 127$) were not significantly different ($P > 0.5$) from those in the wild type (126.3 ± 6.1 μm and 97.4 ± 4.9 μm, respectively; $n = 179$). The number of branch points was also similar (1.75 ± 0.04 μm for *Sema6a*$^{-/-}$ neurons compared to 1.70 ± 0.03 μm for wild type, $P > 0.5$; data not shown).

To assess cell migration more directly, we cultured EGL explants on polylysine and laminin for between 18 h and 4.5 d (ref. 30). In these cultures, granule cells migrate away from the explant in the absence of any radial glia and follow the exact sequence of *in vivo* differentiation. The number of migrating granule cells, quantified using Hoechst staining and phalloidin (**Fig. 6**), in cultures derived from EGL explants

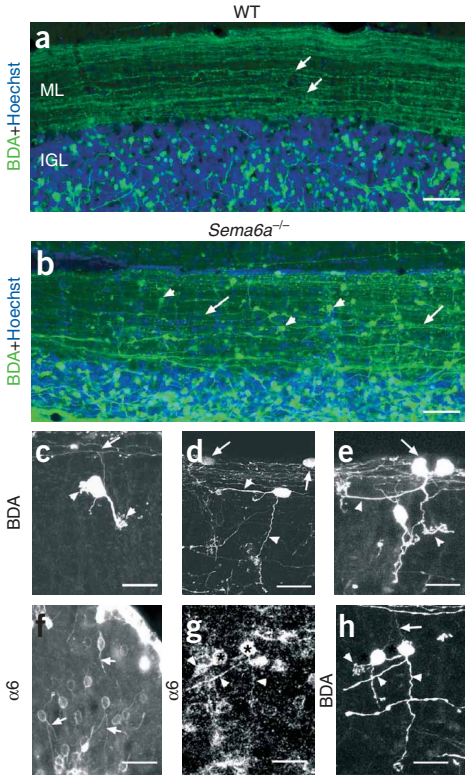

Figure 5 *In vivo* labeling of ectopic granule cells and parallel fibers in *Sema6a*$^{-/-}$. (**a**–**e**,**g**,**h**) Cerebellum sections of wild-type and *Sema6a*$^{-/-}$ adult mice injected with BDA; in **a** and **b**, with Hoechst counterstaining. (**a**,**b**) In wild-type (wt; see **a**) and *Sema6a*$^{-/-}$ (see **b**), BDA labels parallel fibers (arrows in **a** and **b**) in the molecular layer (ML) extending across the mediolateral axis of the injected folia. However, whereas retrogradely labeled granule cell bodies in wt are exclusively found in the IGL, in *Sema6a*$^{-/-}$, many are observed in the ML (arrowheads). Panels **c**–**e**,**g** and **h** are confocal images of ectopic granule cells in the upper part of the molecular layer of *Sema6a*$^{-/-}$ mice. Many ectopic granule cells have a typical morphology with a T-shape axon (arrow in **c** and **h**) and hook-ended dendrites (arrowheads in **c**–**e** and **h**). Other ectopic granule cells close to the pial surface have a more bipolar morphology (arrows in **d** and **e**). These dendrites are also α6-immunoreactive (arrows in **g** and **h**), whereas the axon is not (arrowhead in **h**). (**f**) In adult *Sema6a*$^{-/-}$ cerebellum, most ectopic granule cells extend in the ML α6-positive dendrites (short arrows) oriented toward the IGL. Scale bars, 75 μm (**a**,**b**), 10 μm (**c**,**e**), 20 μm (**d**,**g**,**h**), 35 μm (**f**).

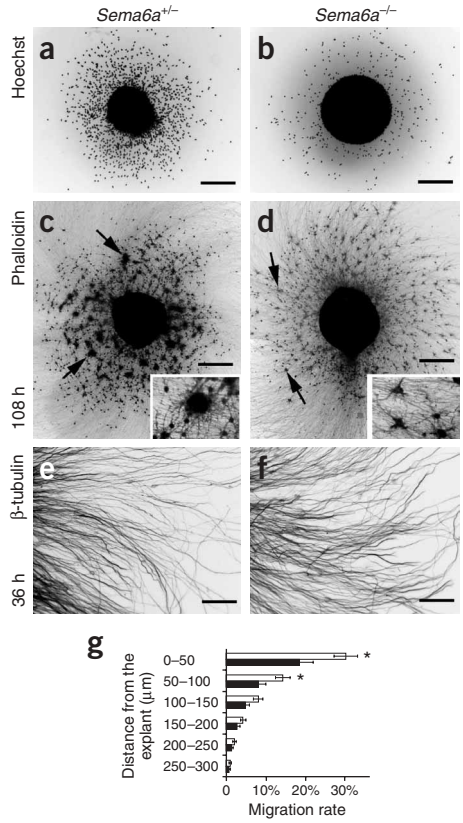

Figure 6 Abnormal *in vitro* migration of Sema6A-deficient granule cells. (**a**–**f**) Migration and neurite outgrowth from P4 EGL microexplants after 36 h (**a**,**b**,**e**,**f**) or 108 h (**c**,**d**). Hoechst staining revealed that after 36 h, there is a significantly lower number of migrating granule cells in *Sema6a*$^{-/-}$ (**b**) compared to *Sema6a*$^{+/-}$ explants (**a**). After 108 h *in vitro*, phalloidin staining shows that migrating granule cells form large aggregates with *Sema6a*$^{+/-}$ explants (arrows in **c**), whereas the aggregates are much smaller with *Sema6a*$^{-/-}$ explants (arrows in **d**). The number of aggregates is also lower. After 36 h *in vitro*, Tuj-1 immunostaining reveals that the number of neurites cutting a line at 150 μm from the explant) was similar in *Sema6a*$^{+/-}$ (see **e**) (367.4 ± 25.3 neurites/mm; $n = 24$) and *Sema6a*$^{-/-}$ (see **f**) explants (379.6 ± 26.3 neurites/mm; $n = 10$). (**g**) Quantification of the distribution of migrating granule cells around EGL explants in *Sema6a*$^{-/-}$ and *Sema6a*$^{+/-}$ (see Methods). The asterisk indicates a significant difference between the two (one-tailed *t*-test; $^*P < 0.05$). Scale bars, 225 μm (**a**–**d**), 55 μm (**e**,**f**).

from Sema6A-deficient mice was considerably reduced after 36 h *in vitro* (**Fig. 6a**,**b**,**g**). After 36 h, the maximum migration distance (the external limit of the region that comprised 90% of the granule cells) was also significantly lower ($P = 0.02$) for the *Sema6a*$^{-/-}$ granule cells (127.9 ± 12.4 μm; $n = 5$) than for the *Sema6a*$^{+/-}$ granule cells (189 ± 17.1 μm; $n = 6$) . After 4.5 d in culture, most granule cells from wild-type mice aggregated, forming large clusters (**Fig. 6c**). With explants from *Sema6a*$^{-/-}$ cerebellum, aggregates formed but their number and size were smaller (**Fig. 6d**). The timing of TAG-1 and MAP2 expression was similar in wild-type and *Sema6a*$^{-/-}$ EGL cultures, showing that the absence of Sema6A does not affect granule cell maturation (data not shown). Notably, the number of processes growing from EGL explants (**Fig. 6e**,**f**) was similar in *Sema6a*$^{+/-}$ and *Sema6a*$^{-/-}$. Finally, wild-type EGL explants were cultured on Sema6A substrate ($n = 23$) or in a medium containing Sema6A-Fc ($n = 27$; see Methods) for between 36 and 96 h. In both conditions, the number of migrating granule cells and granule cell clusters were unchanged (**Supplementary Fig. 3**).

These results suggested that, in the absence of Sema6A, granule cells could extend normal processes but that the movements of the nucleus, soma, or both were perturbed. To confirm this, we performed time-lapse videomicroscopy on EGL explants after 24–48 h in cultures (**Fig. 7a**,**b**). In control explants ($n = 3$ explants; two independent experiments), migrating cells rapidly extended a long leading process bearing typical growth cones away from the explant. A large enlargement at the rear contained the nucleus (**Supplementary Video 1** online and **Fig. 7a**). Time-lapse videomicroscopy showed that nuclear movement was saltatory and was preceded by the appearance of an elongated swelling ahead of the nucleus, such as has recently been described for cortical interneurons[31] (**Supplementary Video 2** online and **Fig. 7a**). Although the nucleus was often stationary, the overall movement of the cell body was always in the opposite direction from the explant core. In

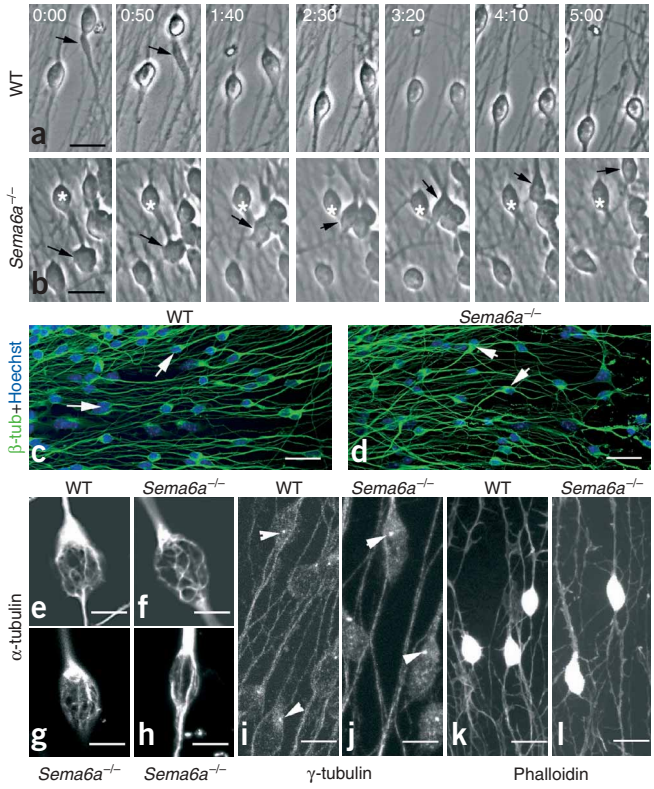

Figure 7 Abnormal granule cell movement in absence of Sema6A. (**a**,**b**) Time-lapse imaging of granule cell migration from P5 EGL microexplants cultured for 24 h before imaging. Explants are located on the top of the frame (interval between pictures is 50 min). In wild-type (see **a**), granule cells migrate opposite to the explant. They transiently show an elongated swelling just ahead of the nucleus (arrow). In contrast, most *Sema6a*$^{-/-}$ granule cells (see **b**) remains stationary (asterisk) or move back toward the explant (arrow). (**c**–**h**) α-tubulin immunostaining of wild-type (**c**,**e**) or *Sema6a*$^{-/-}$ (**d**,**f**–**h**) EGL microexplants cultured for 36 h (with Hoechst counterstaining). Explants are on the left side of the frame for **c** and **d** and in the bottom for **e**–**h**. Many migrating *Sema6A*$^{-/-}$ granule cells (arrows in **d**) appear misoriented compared to wild type (arrows in **c**). However, the perinuclear cage of microtubule labeled with antibody to α-tubulin appears similar in granule cells from wild-type (see **e**) and Sema6A-deficient (**f**–**h**) mice. (**i**,**j**) γ-tubulin immunostaining of the centrosome in granule cells migrating from EGL explants. In granule cells derived from both wild-type (**i**) and *Sema6a*$^{-/-}$ mice (**j**), the centrosome is positioned ahead of the nucleus. (**k**,**l**) Phalloidin-FITC staining of the actin cytoskeleton in granule cells migrating from EGL explants. No difference is observed between wild-type (**i**) and *Sema6a*$^{-/-}$ (**j**). Scale bars, 25 μm (**a**,**b**,**k**,**l**), 30 μm (**c**,**d**), 6 μm (**e**–**h**), 15 μm (**i**,**j**).

explants from Sema6A-deficient mice ($n = 8$ explants; three independent experiments), long leading processes with very dynamic growth cones were also observed, suggesting that neurite extension was normal (**Fig. 7b** and **Supplementary Video 3** online). However, the forward movement of the nucleus was perturbed. Most cell bodies appeared to oscillate without moving substantially. Furthermore, cells migrating toward the explant were always observed (**Supplementary Videos 3–5** and **Fig. 7b**). Finally, in the vicinity of the explants, cell bodies seemed more tightly aggregated than in the wild type.

To further characterize this abnormal migration, EGL cultures at 36 h were fixed and labeled with markers of the cytoskeleton and centrosome that are important components of the migration machinery[31,32]. The overall disorganization of the cohort of migrating granule cells was clearly observed using α-tubulin staining (**Fig. 7c**,**d**). However, the perinuclear cage of microtubules[32] appeared similar in wild-type and Sema6A-deficient cells (**Fig. 7e–h**). The centrosome could also be observed using antibodies to γ-tubulin[32]; it had a comparable position in the wild-type and Sema6A-deficient cells (**Fig. 7i**,**j**). Finally, the actin cytoskeleton labeled with phalloidin appeared similar in wild-type and Sema6A-deficient granule cells (**Fig. 7k**,**l**).

Non-cell-autonomous function of Sema6A in granule cells

Sema6D and insect class I semaphorins act as ligands and receptors[10,12]. To determine whether Sema6A functions as a receptor or as a ligand in migrating granule cells, we generated mouse chimeras. Sema6A mutant mice were first crossed with mice expressing green fluorescent protein (GFP) attached to the chicken *Actb* (β-actin) promoter (*Actb-GFP* mice)[33] to allow the cells of each genotype to be distinguished (see Methods). *GFP;Sema6a*$^{-/-}$morulae were then aggregated to wild-type ('wt') morulae to obtain *GFP;Sema6a*$^{-/-}$*:wt* chimeric mice ($n = 2$). As a control, we also obtained *GFP;Sema6a*$^{+/-}$*:wt* chimeras ($n = 5$). The proportion of Sema6A-deficient cells, as determined on the basis of GFP expression, was between 30% and 40% ($n = 2$). GFP was detected in all types of cerebellar cells such as Bergmann glia and Purkinje cells (**Fig. 8** and data not shown). In *GFP;Sema6a*$^{+/-}$*:wt* chimeras, no

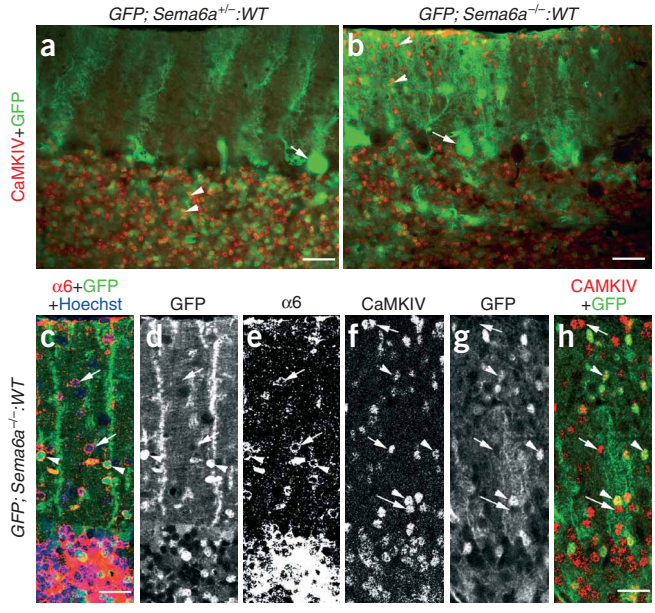

Figure 8 Non-cell-autonomous function of Sema6A in migrating granule cells. (**a**–**h**) Cerebellum sections from *GFP; Sema6a*$^{+/-}$*:wt* (in **a**) and *GFP; Sema6a*$^{-/-}$*:wt* (in **b**–**h**) mouse chimeras labeled with antibody to GFP (**a**–**d**,**g**,**h**) and CaMKIV (**a**,**b**,**f**,**h**), or α6 (**c**,**e**). In *GFP; Sema6a*$^{+/-}$*:wt* chimera (see **a**), all CaMKIV- and GFP-positive granule cells (arrowheads) are in the IGL. Some Purkinje cells also express GFP (arrow). In contrast, in *GFP; Sema6a*$^{-/-}$*:wt* chimera (see **b**), many CaMKIV-positive ectopic granule cells are observed in the molecular layer (arrowheads). (**c**–**h**) 4-μm confocal images of cerebellum sections from *GFP; Sema6a*$^{-/-}$*:wt* chimera labeled with α6 (in **c** and **e**), CaMKIV (**f**,**h**) and GFP. Many α6- or CaMKIV-positive granule cells are located in ML. Only a subset of these ectopic granule cells are GFP positive (and thus *Sema6a*$^{-/-}$; arrowheads), and the majority are GFP negative (and thus of wild-type origin; arrows). Scale bars, 75 μm (**a**,**b**), 35 μm (**c**–**h**).

ectopic α6- or CaMKIV-positive cells were detected in the molecular layer (**Fig. 8a**). In contrast, many ectopic CaMKIV- and α6-positive granule cells were detected in the molecular layer of *GFP;Sema6a*$^{-/-}$*:wt* (**Fig. 8b,c**). Among GFP-expressing granule cells, about 30% were ectopic. Confocal microscopy analysis revealed that only a minority—about 30–40%—of the CaMKIV- and α6-positive ectopic cells were also GFP positive and thus deficient in Sema6A (**Fig. 8c–h**). These cells were dispersed throughout the molecular layer. The remaining α6-positive ectopic cells were GFP negative, and thus of wild-type origin; like the GFP-positive cells, these were homogeneously distributed in the molecular layer.

DISCUSSION

It has been proposed that each phase of granule cell development is controlled by both extrinsic factors and an intrinsic developmental program[34]. Some factors acting on granule cells within the EGL have begun to be identified. Thus, the bHLH transcription factor Math1 is necessary for lineage determination of granule cells[35]. In the outer EGL, the proliferation of granule cell progenitors requires Purkinje cell–derived Sonic hedgehog[36]. The passage from the outer EGL to the deeper EGL involves the chemokine stromal-derived factor-1 and EphB2-ephrinB2 reverse signaling[37]. The initiation of granule cell axon elongation in the deeper EGL is regulated by interaction between the serine/threonine kinase Unc51.1, SynGAP and syntenin[38]. Finally, many extracellular cues—such as glutamate[39], neuregulin[40] and BDNF[41]—modulate the radial migration of granule cells and may cooperate with Sema6A to trigger migration.

However, Sema6A function differs from these factors in that proliferation, migration to the deeper EGL and parallel fiber extension are normal in *Sema6a*$^{-/-}$ mice. Our data, together with previous anatomical[2,4] and time-lapse analyses[3], show that Sema6A is expressed by tangentially migrating granule cells in the deep EGL and is turned off when they initiate radial migration. Sema6A function seems to be specifically required for the initiation of radial migration. We favor a model (**Supplementary Fig. 4** online) in which Sema6A regulates interactions between granule cells, rather than with Bergmann glia. First, Sema6A is no longer expressed by granule cells when this interaction occurs and is never expressed by Bergmann glia, whose morphology appears normal in *Sema6a*$^{-/-}$ mutants. Second, granule cell migration from EGL explants *in vitro*, which occurs without Bergmann glia, is abnormal in absence of Sema6A. Notably, Sema6A does not affect granule cell neurite outgrowth *in vitro* and *in vivo*, which might have been its expected role. Our observations suggest, rather, that Sema6A is specifically involved in the early steps of nuclear and soma translocation within the radially oriented granule cell processes (**Supplementary Fig. 4**). Thus, Sema6A function differs from that of other known molecules expressed in the deeper EGL (such as Unc51.1 and Pax6) that principally control parallel fiber extension.

Drosophila Sema1a, which is closely related to class 6 semaphorins, seems capable of acting as a receptor[12], and Sema6D can act as a receptor for plexin-A1 (ref. 10). However, the analysis of Sema6A chimeras reveals that Sema6A function in the EGL is primarily non-cell-autonomous. This does not rule out a possible receptor function for Sema6A at certain time-points or in other neurons. The best candidate receptors for Sema6A on granule cells are type A plexins[9,10], one of which—plexin-A4—mediates Sema6A repulsive activity on sympathetic axons. However, plexin-A4 *mRNA* was not detected in the developing cerebellar cortex (unpublished data).

Sema6A does not seem to be cleaved and thus may work as a contact repellent, providing spatial information for underlying cells in the deeper EGL—in particular, for radially migrating cells; thus Sema6A, together with gradients of secreted factors[37], may serve to orient granule cell migration away from the EGL (**Supplementary Fig. 4**). This is consistent with the failure of many granule cells to migrate away from the EGL in Sema6A mutants and with the observations, from time-lapse videomicroscopy, that many granule cells from Sema6A-mutant explants migrate in the wrong direction (towards the explant). Accordingly, the perturbation of this spatial information may also explain the presence of many ectopic wild-type granule cells in *Sema6a*$^{-/-}$*:wt* chimeras. However, the extinction of Sema6A expression with the initiation of radial migration also suggests that the spatiotemporal control of Sema6A expression provides a carefully regulated paracrine signal that may initiate radial migration or arrest tangential migration.

An alternative hypothesis is that Sema6A primarily controls the level of adhesion between tangentially migrating cells and that the defects in the initiation of radial migration are secondary to increased adhesion between granule cells in the absence of Sema6A function. Sema1A has been shown to affect defasciculation of motor axons at discrete choice points[42] by countering the attractive activity of homophilic proteins. Notably, in *Sema6a*$^{-/-}$ mice, many ectopic granule cells are clustered near the pial surface, and the motility of granule cell bodies is also markedly reduced in EGL cultures. Thus, Sema6A could function as a de-adhesive molecule in tangentially migrating granule cells, facilitating, through contact repulsion, granule cell movement in the EGL and the response to another signal to initiate radial migration. However, in EGL explant cultures, the Sema6A ectodomain does not seem to influence granule cell migration and clustering.

Our time-lapse imaging experiments showed that the primary consequence of Sema6A deficiency is a defect in the translocation of the granule cell soma or nucleus. Oriented nuclear translocation, or nucleokinesis, has been described in most migrating neurons and in other cell types[31,32,43]. Migrating neurons are highly polarized, with cytoplasmic organelles such as the centrosome and the Golgi apparatus at their leading edge, and the nucleus at their rear. We could not detect any obvious defects in the centrosome or cytoskeleton in *Sema6a*$^{-/-}$ granule cells, suggesting that their abnormal migration may not result from a major disorganization of the migration machinery. It will be important to determine whether the expression or function of the centrosomal components is altered, and in particular those of Par6α, which regulates cytoskeletal dynamics and nucleokinesis in radially migrating granule cells[32].

Many other questions remain unanswered. Sema6A mRNA is expressed in granule cells in the IGL, although these cells are not immunoreactive with Sema6A. This shows that the expression of Sema6A protein is developmentally regulated and subject to precise translational modifications, post-translational modifications or both. The defects in initiation and orientation of granule cell migration suggest that the regulation of Sema6A protein expression provides a precise spatiotemporal signal. In addition, the observation that about 60% of granule cells are still able to reach the IGL suggests either that granule cells are heterogeneous or that other molecules act together with Sema6A to control the transition from tangential to radial migration.

Sema6A-deficient mice also provide a good model for studying other aspects of cerebellar development. During development, mossy fibers never invade the molecular layer and remain below the Purkinje cells[44]. *In vitro* experiments have also suggested that mossy fiber growth is regulated by target-derived stop signals produced by granule cells, and by inhibitory signals produced by Purkinje cells or present in the molecular layer[16]. In *Sema6a*$^{-/-}$ mice, ectopic granule cells in the molecular layer differentiate and receive mossy fiber innervation. Thus,

the unusual cellular environment does not preclude an intrinsic differentiation program. In addition to, and together with, other previous examples of mossy fiber contacts observed on ectopic granule cells in wild-type mice or as a result of 6-hydroxydopamine treatments[45,46], this result shows that there are no inhibitors that prevent mossy fibers from entering the molecular layer. Rather, the surprising capacity of mossy fibers to find and contact granule cells far from the IGL suggests that granule cells secrete long-range chemoattractants for mossy fibers.

METHODS

Animals. Swiss and C57/Bl6 mice (Janvier) were used for expression studies. The Sema6A-deficient line has been previously described[13]: briefly, a cassette encoding CD4 transmembrane domain–β-galactosidase–neomycin phosphotransferase (TM-β-geo) and human placental alkaline phosphatase (PLAP), separated by an internal ribosome entry site (IRES), was inserted in the 17th intron of Sema6A[14]. The remaining N-terminal portion of the Sema6A protein up to amino acid 623 (and thus lacking the transmembrane and cytoplasmic domains) was fused to β-galactosidase and trapped in the endoplasmic reticulum (see Results). *GFP;Sema6a* mice were obtained by crossing Sema6A-deficient mice with transgenic mice expressing GFP under the chicken β-actin promoter[33].

P0–P5 mice were anesthetized on ice and, after P5, by inhalation of isofluorane Foren (Abbott). The day of birth corresponds to P0. All animal procedures were carried out in accordance with institutional guidelines.

Genotyping of Sema6A-deficient mice. DNA were prepared from tails using the Red Extract-N-Amp Tissue PCR kit (Sigma). The Sema6A genotype was determined by PCR using the following primers: 5′-GAG ATG CAC AGC TAA CTT CTG GTG-3′ (wild-type allele forward primer), 5′-TTG AAG CCT GCT CTT AGT GGC TCC-3′ (reverse primer) and 5′-GCT ACC GGC TAA AAC TTG AGA CCT-3′ (mutant allele reverse primer), which amplified a 1.43-kb product for the wild-type allele and a 990-kb product for the mutant allele.

Immunocytochemistry. Brains were collected as has been previously described[47]. Brain sections were incubated with antibodies against hSema6A (1:200 ; R&D Systems), mSema6A (1:200; R&D Systems), β−galactosidase (1:1,000; Cappel), $GABA_A$ receptor α6 subunit (1:1,000; Chemicon), CaMKIV (1:500), TAG-1 (TG1; 1:3000), L1 (1:100; Chemicon), Pax6 (1:1,000; Chemicon), CaBP (1:1,000; SWANT), parvalbumin (1:1,000; Sigma), zebrin II Q113 (1:500), GFAP (1:400; Chemicon), VGLUT2 (1:3,000; Chemicon), phosphohistone-H3 (1:1,000; Cell Signaling), activated caspase-3 (1:250; Cell Signaling), Dcx (1:1,000; Chemicon), fibronectin (1:500; Sigma), GFP (1:300; Molecular Probes), GFP (1:200; US Biological) or NCL-Ki67 (1:1,000; Novocastra) followed by species-specific secondary antibodies (Jackson ImmunoResearch). Sections were counterstained with Hoechst 33258 (10 μg/ml, Sigma), mounted in Mowiol (Calbiochem) and examined with a fluorescence microscope (DMR, Leica) or a fluorescence confocal microscope (DM IRBE, Leica). Deconvolution was performed by the 3D deconvolution module from Metamorph 6.2r2 software (Universal Imaging Corp.).

BrdU injections and staining. P7 and P10 mice were injected intraperitoneally with BrdU (Sigma; 15 mg/ml, 50 mg per kg of body weight) diluted in a saline solution. Animals were perfused 3 h or 108 h after injection. Brain sections were incubated with a rat antibody to BrdU (1:100; Harlan).

***In situ* hybridization.** Antisense riboprobes were labeled as described previously[47] by *in vitro* transcription of cDNAs encoding mouse *Math1* (gift from M. Wassef[48]), *Barlh1* (gift from F. Qiu[21]) or *Sema6a*[15]. *In situ* hybridization was done as described[47].

BDA injections. Adult mice were anesthetized with ketamine (Imalgene 500, 146 mg/kg; Merial) and xylazine (Rompun 2%, 7.4 mg/kg; Bayer), after which 1 μl of 10% biotin-dextran (BDA; 10,000 MW; Molecular Probes) was injected into the cerebellum with a glass micropipet. Mice were killed 48 h later. BDA was revealed with CY3-conjugated streptavidin (1:400; Jackson Immunoresearch).

Generation of chimeric animals. To obtain chimeras between *GFP;Sema6a*$^{-/-}$ and wild-type cells, morulae from *GFP;Sema6a*$^{-/-}$ × *GFP;Sema6a*$^{-/-}$ crosses were aggregated *in vitro* with morulae of wild-type mice. As controls, we aggregated morulae from wild-type mice with those from *GFP;Sema6a*$^{-/-}$ × *GFP;Sema6a*$^{+/+}$ crosses. Morula aggregation was performed as has been previously described[49], with a few modifications. Briefly, after removal of the zona pellucida, two morulae of appropriate genotypes were put in contact in a drop of 100 μg/ml phytohemagglutinin PHA-P (Sigma) in PBS, until they were physically attached (about 1 min). The embryo pairs were then transferred into depression wells containing M16 medium (Sigma). After overnight culture at 37 °C in 7% CO_2, blastocysts resulting from aggregations were transferred into pseudopregnant C57Bl/6/CBA females.

Dissociated granule cell cultures. Granule cells were purified as has been previously described[50] and plated onto polylysine (0.2 mg/ml; Sigma) and laminin (20 μg/ml; Sigma), onto COS7 cells, or onto COS7 cells transfected with full-length Sema6A, in culture medium (BME (Invitrogen), 0.45% glucose, 10% horse serum, 5% fetal bovine serum (Eurobio)). Cultures were fixed after 24 or 48 h with 4% paraformaldehyde (PFA), 0.33 M sucrose and immunostained with mouse antibody to β-tubulin (Tuj-1: 1:1,000; Eurogentec).

Microexplants culture. Microexplants cultures of P4 or P5 mice were prepared as described previously[30]. Cultures were fixed after 18, 36, 72, 96 or 108 h with 4% PFA, 0.33 M sucrose. To test Sema6A activity, EGL explants were cultured on polylysine (0.2 mg ml^{-1}; Sigma), laminin (10 μg/ml or 20 μg/ml) and recombinant Sema6-Fc (R&D Systems; 1,000 μg/ml) or in culture medium containing 1,000 ng/ml of Sema6A-Fc preclustered with antibody to human IgG1 (Jackson ImmunoResearch). Cultures were stained with phalloidin (Sigma) or immunostained with mouse antibody to β-tubulin or mouse antibody to α-tubulin (1:1,000; Sigma) and counterstained with Hoechst 33342 (10 μg/ml, Sigma). For centrosome stainings, cultures were fixed 10 min in −20 °C methanol and immunostained with rabbit antibody to γ-tubulin (1:500; Sigma).

Migration and outgrowth analysis. Analysis was performed with Metamorph. To measure migration rates, we delimited concentric areas of 50-μm width at increasing distances from the explant border. The number of Hoechst-labeled pixels within each area was counted and then expressed as a percentage of the total number of pixels. To evaluate the overall rate of neuronal migration, the total number of Hoechst-labeled pixels surrounding each half of the explant was counted. The number of clusters (containing a minimum of five cells) surrounding the explant was also counted.

Maximal neurite length were estimated by measuring the three longest Tuj-1–positive neurites of each explant. Neuritic length was estimated by laying out a circle containing approximately 90% of the Tuj-1–positive neurites. We also counted the total number of Tuj-1–positive neurites within the 150-μm perimeter around the explant border.

Time-lapse videomicroscopy. EGL microexplants were cultured 24–48 h as described below, in Petri dishes equipped with glass coverslips. Before imaging, 20 mM HEPES was added to the culture medium. Pictures were acquired with an inverted microscope (DM IRBE, Leica) equipped with a Micromax CDD Princeton camera driven with Metamorph Software. Pictures were captured every 5 min using a ×20 dry objective equipped with phase optics, in a 37 °C chamber. Hoechst 33342 was added to culture medium ($1:10^6$; Sigma) to visualize the nucleus in live cells.

Cresyl violet staining. Sections were colored 7 min in a 1% cresyl violet and 1% thionine solution and then differentiated in 80% ethanol and acetic acid.

Western blotting. COS7 cells were transfected with Lipofectamine2000 (Invitrogen). Cell extracts were collected 48 h later, separated by SDS-PAGE and western blotted by standard methods. Proteins were immunodetected with antibodies to mSema6A (1:500; R&D Systems), hSema6A (1:250; R&D Systems), hSema6A (1:500; R&D Systems) or myc E910 (1:200; Santa Cruz), followed by horseradish peroxidase–linked secondary antibodies and ECL kit (Amersham).

Statistical analysis. For all statistical analysis, the significance was calculated by ANOVA (Statview, Abacus Concepts).

Note: Supplementary information is available on the Nature Neuroscience website.

ACKNOWLEDGMENTS

We thank C. Sotelo for his constant support and comments on the manuscript; H. Sakagami and H. Kondo (Tohoku University) for anti-β isoform of CaMKIV antibody; R. Hawkes (University of Calgary, Canada) for Zebrin II Q113 antibody; D. Karagogeos (University of Crete, Greece) for TAG-1 antibody; F. Qiu (UMDNJ, Piscataway, USA) for *Barhl1* cDNA; M. Wassef (ENS, Paris, France) for *Math1* cDNA; K. Skurka and D. Rottkamp for help in localizing the insertion site in the *Sema6a* gene trap allele; R. Schwartzmann and V. Georget (Service d'Imagerie IFR83, Université Paris 6, France) for their help with confocal and videomicroscopy studies; and M. Wassef, C. Lebrand, C. Métin and J.P. Baudoin for discussions. A.C. is supported by the Fondation pour la Recherche sur le Cerveau (FRC), the Schlumberger Foundation and the Association pour la Recherche sur le Cancer (ARC). K.J.M is a Science Foundation Ireland (SFI) Investigator. This work was supported by SFI grant 01/F.1/B006 to K.J.M; and grants from the 21st Century COE Program, and from the Core Research for Evolutional Science and Technology (CREST) of the Japan Science and Technology Agency (JST) to H.F.

COMPETING INTERESTS STATEMENT

The authors declare that they have no competing financial interests.

Published online at http://www.nature.com/natureneuroscience/
Reprints and permissions information is available online at http://npg.nature.com/reprintsandpermissions/

1. Wingate, R.J. The rhombic lip and early cerebellar development. *Curr. Opin. Neurobiol.* **11**, 82–88 (2001).
2. Ryder, E.F. & Cepko, C.L. Migration patterns of clonally related granule cells and their progenitors in the developing chick cerebellum. *Neuron* **12**, 1011–1028 (1994).
3. Komuro, H., Yacubova, E. & Rakic, P. Mode and tempo of tangential cell migration in the cerebellar external granular layer. *J. Neurosci.* **21**, 527–540 (2001).
4. Ramon y Cajal, S. *Histologie du système nerveux de l'homme et des vertébrés* (Maloine, Paris, 1911).
5. Yacubova, E. & Komuro, H. Cellular and molecular mechanisms of cerebellar granule cell migration. *Cell Biochem. Biophys.* **37**, 213–234 (2003).
6. Fiore, R. & Puschel, A.W. The function of semaphorins during nervous system development. *Front. Biosci.* **8**, s484–s499 (2003).
7. Qu, X. *et al.* Identification, characterization, and functional study of the two novel human members of the semaphorin gene family. *J. Biol. Chem.* **277**, 35574–35585 (2002).
8. Kikuchi, K. *et al.* Cloning and characterization of a novel class VI semaphorin, semaphorin Y. *Mol. Cell. Neurosci.* **13**, 9–23 (1999).
9. Suto, F. *et al.* Plexin-a4 mediates axon-repulsive activities of both secreted and transmembrane semaphorins and plays roles in nerve fiber guidance. *J. Neurosci.* **25**, 3628–3637 (2005).
10. Toyofuku, T. *et al.* Guidance of myocardial patterning in cardiac development by Sema6D reverse signalling. *Nat. Cell. Biol.* (2004).
11. Winberg, M.L. *et al.* Plexin A is a neuronal semaphorin receptor that controls axon guidance. *Cell* **95**, 903–916 (1998).
12. Godenschwege, T.A., Hu, H., Shan-Crofts, X., Goodman, C.S. & Murphey, R.K. Bi-directional signaling by Semaphorin 1a during central synapse formation in *Drosophila*. *Nat. Neurosci.* **5**, 1294–1301 (2002).
13. Leighton, P.A. *et al.* Defining brain wiring patterns and mechanisms through gene trapping in mice. *Nature* **410**, 174–179 (2001).
14. Mitchell, K.J. *et al.* Functional analysis of secreted and transmembrane proteins critical to mouse development. *Nat. Genet.* **28**, 241–249 (2001).
15. Zhou, L. *et al.* Cloning and expression of a novel murine semaphorin with structural similarity to insect semaphorin I. *Mol. Cell. Neurosci.* **9**, 26–41 (1997).
16. Rabacchi, S.A. *et al.* Collapsin-1/semaphorin-III/D is regulated developmentally in Purkinje cells and collapses pontocerebellar mossy fiber neuronal growth cones. *J. Neurosci.* **19**, 4437–4448 (1999).
17. Fujita, S., Shimada, M. & Nakamura, T. H3-thymidine autoradiographic studies on the cell proliferation and differentiation in the external and the internal granular layers of the mouse cerebellum. *J. Comp. Neurol.* **128**, 191–208 (1966).
18. Nusser, Z., Sieghart, W. & Somogyi, P. Segregation of different GABAA receptors to synaptic and extrasynaptic membranes of cerebellar granule cells. *J. Neurosci.* **18**, 1693–1703 (1998).
19. Sakagami, H., Umemiya, M., Kobayashi, T., Saito, S. & Kondo, H. Immunological evidence that the beta isoform of Ca^{2+}/calmodulin-dependent protein kinase IV is a cerebellar granule cell-specific product of the CaM kinase IV gene. *Eur. J. Neurosci.* **11**, 2531–2536 (1999).
20. Ahn, A.H., Dziennis, S., Hawkes, R. & Herrup, K. The cloning of zebrin II reveals its identity with aldolase C. *Development* **120**, 2081–2090 (1994).
21. Li, S., Qiu, F., Xu, A., Price, S.M. & Xiang, M. Barhl1 regulates migration and survival of cerebellar granule cells by controlling expression of the neurotrophin-3 gene. *J. Neurosci.* **24**, 3104–3114 (2004).
22. Wood, K.A., Dipasquale, B. & Youle, R.J. *In situ* labeling of granule cells for apoptosis-associated DNA fragmentation reveals different mechanisms of cell loss in developing cerebellum. *Neuron* **11**, 621–632 (1993).
23. Matsunaga, E. *et al.* RGM and its receptor neogenin regulate neuronal survival. *Nat. Cell. Biol.* **6**, 749–755 (2004).
24. Kyriakopoulou, K., de Diego, I., Wassef, M. & Karagogeos, D. A combination of chain and neurophilic migration involving the adhesion molecule TAG-1 in the caudal medulla. *Development* **129**, 287–296 (2002).
25. Lindner, J., Rathjen, F.G. & Schachner, M. L1 mono- and polyclonal antibodies modify cell migration in early postnatal mouse cerebellum. *Nature* **305**, 427–430 (1983).
26. Gleeson, J.G., Lin, P.T., Flanagan, L.A. & Walsh, C.A. Doublecortin is a microtubule-associated protein and is expressed widely by migrating neurons. *Neuron* **23**, 257–271 (1999).
27. Chan-Palay, V. Arrested granule cells and their synapses with mossy fibers in the molecular layer of the cerebellar cortex. *Z. Anat. Entwicklungsgesch.* **139**, 11–20 (1972).
28. Hioki, H. *et al.* Differential distribution of vesicular glutamate transporters in the rat cerebellar cortex. *Neuroscience* **117**, 1–6 (2003).
29. Soha, J.M., Kim, S., Crandall, J.E. & Vogel, M.W. Rapid growth of parallel fibers in the cerebella of normal and staggerer mutant mice. *J. Comp. Neurol.* **389**, 642–654 (1997).
30. Nagata, I. & Nakatsuji, N. Granule cell behavior on laminin in cerebellar microexplant cultures. *Brain Res. Dev. Brain Res.* **52**, 63–73 (1990).
31. Bellion, A., Baudoin, J.P., Alvarez, C., Bornens, M. & Metin, C. Nucleokinesis in tangentially migrating neurons comprises two alternating phases: forward migration of the Golgi/centrosome associated with centrosome splitting and myosin contraction at the rear. *J. Neurosci.* **25**, 5691–5699 (2005).
32. Solecki, D.J., Model, L., Gaetz, J., Kapoor, T.M. & Hatten, M.E. Par6alpha signaling controls glial-guided neuronal migration. *Nat. Neurosci.* **7**, 1195–1203 (2004).
33. Hadjantonakis, A.K., Gertsenstein, M., Ikawa, M., Okabe, M. & Nagy, A. Generating green fluorescent mice by germline transmission of green fluorescent ES cells. *Mech. Dev.* **76**, 79–90 (1998).
34. Yacubova, E. & Komuro, H. Intrinsic program for migration of cerebellar granule cells in vitro. *J. Neurosci.* **22**, 5966–5981 (2002).
35. Jensen, P., Smeyne, R. & Goldowitz, D. Analysis of cerebellar development in math1 null embryos and chimeras. *J. Neurosci.* **24**, 2202–2211 (2004).
36. Wechsler-Reya, R.J. & Scott, M.P. Control of neuronal precursor proliferation in the cerebellum by Sonic Hedgehog. *Neuron* **22**, 103–114 (1999).
37. Lu, Q., Sun, E.E., Klein, R.S. & Flanagan, J.G. Ephrin-B reverse signaling is mediated by a novel PDZ-RGS protein and selectively inhibits G protein-coupled chemoattraction. *Cell* **105**, 69–79 (2001).
38. Tomoda, T., Kim, J.H., Zhan, C. & Hatten, M.E. Role of Unc51.1 and its binding partners in CNS axon outgrowth. *Genes Dev.* **18**, 541–558 (2004).
39. Komuro, H. & Rakic, P. Modulation of neuronal migration by NMDA receptors. *Science* **260**, 95–97 (1993).
40. Rio, C., Rieff, H.I., Qi, P., Khurana, T.S. & Corfas, G. Neuregulin and erbB receptors play a critical role in neuronal migration. *Neuron* **19**, 39–50 (1997).
41. Borghesani, P.R. *et al.* BDNF stimulates migration of cerebellar granule cells. *Development* **129**, 1435–1442 (2002).
42. Yu, H.H., Huang, A.S. & Kolodkin, A.L. Semaphorin-1a acts in concert with the cell adhesion molecules fasciclin II and connectin to regulate axon fasciculation in Drosophila. *Genetics* **156**, 723–731 (2000).
43. Gomes, E.R., Jani, S. & Gundersen, G.G. Nuclear movement regulated by Cdc42, MRCK, myosin, and actin flow establishes MTOC polarization in migrating cells. *Cell* **121**, 451–463 (2005).
44. Arsenio Nunes, M.L. & Sotelo, C. Development of the spinocerebellar system in the postnatal rat. *J. Comp. Neurol.* **237**, 291–306 (1985).
45. Sievers, J., Mangold, U. & Berry, M. 6-OHDA-induced ectopia of external granule cells in the subarachnoid space covering the cerebellum. III. Morphology and synaptic organization of ectopic cerebellar neurons: a scanning and transmission electron microscopic study. *J. Comp. Neurol.* **232**, 319–330 (1985).
46. Berciano, M.T. & Lafarga, M. Colony-forming ectopic granule cells in the cerebellar primary fissure of normal adult rats: a morphologic and morphometric study. *Brain Res.* **439**, 169–178 (1988).
47. Marillat, V. *et al.* Spatiotemporal expression patterns of slit and robo genes in the rat brain. *J. Comp. Neurol.* **442**, 130–155 (2002).
48. Louvi, A., Alexandre, P., Metin, C., Wurst, W. & Wassef, M. The isthmic neuroepithelium is essential for cerebellar midline fusion. *Development* **130**, 5319–5330 (2003).
49. Hogan, B., Beddington, R.S., Costantini, F. & Lacy, E. *Manipulating the Mouse Embryo: A Laboratory Manual* (Cold Spring Harbor Laboratory Press, Cold Spring Harbor, New York, 1994).
50. Hatten, M.E. Neuronal regulation of astroglial morphology and proliferation *in vitro*. *J. Cell Biol.* **100**, 384–396 (1985).